Neuroscience 145 (2007) 832–840

ENVIRONMENTAL ENRICHMENT SELECTIVELY INCREASES GLUTAMATERGIC RESPONSES IN LAYER II/III OF THE AUDITORY CORTEX OF THE RAT

J. A. NICHOLS, V. P. JAKKAMSETTI, H. SALGADO, L. DINH, M. P. KILGARD AND M. ATZORI*

School for Behavioral and Brain Sciences, The University of Texas at Dallas, 2601 North Floyd Road, GR41, Richardson, TX 75080, USA

Abstract—Prolonged exposure to environmental enrichment (EE) induces behavioral adaptation accompanied by detectable morphological and physiological changes. Auditory EE is associated with an increased auditory evoked potential (AEP) and increased auditory gating in the primary auditory cortex. We sought physiological correlates to such changes by comparing synaptic currents in control vs. EE-raised rats, in a primary auditory cortex (AI) slice preparation. Pharmacologically isolated glutamatergic or $GABA_A$-receptor-mediated currents were measured using perforated patch whole-cell recordings. Glutamatergic AMPA receptor (AMPAR)-mediated excitatory postsynaptic currents (EPSCs) displayed a large amplitude increase (64±11% in EE vs. control) accompanied by a rise-time decrease (−29±6% in EE vs. control) and decrease in pair pulse ratio in layer II/III but not in layer V. Changes in glutamatergic signaling were not associated with changes in the ratio between *N*-methyl-D aspartate-receptor (NMDAR)-mediated vs. AMPAR-mediated components, in amplitude or pair pulse ratio of GABAergic transmission, or in passive neuronal properties.

A realistic computational model was used for integrating *in vivo* and *in vitro* results, and for determining how EE synapses correct for phase error of the inputs. We found that EE not only increases the mean firing frequency of the responses, but also improves the robustness of auditory processing by decreasing the dependence of the output firing on the phase difference of the input signals.

We conclude that behavioral and electrophysiological differences detected *in vivo* in rats exposed to an auditory EE are accompanied and possibly caused by selective changes in cortical excitatory transmission. Our data suggest that auditory EE selectively enhances excitatory glutamatergic synaptic transmission in layer II/III without greatly altering inhibitory GABAergic transmission.

Key words: behavior, AI, patch-clamp, perforated patch, excitation/inhibition balance, neuronal modeling.

*Corresponding author. Tel: +1-972-883-4311; fax: +1-972-883-2491.
E-mail address: marco.atzori@utdallas.edu (M. Atzori).

Abbreviations: ACSF, artificial cerebrospinal fluid; AEP, auditory evoked potential; AMPAR, AMPA receptor; APV, D-2-amino-5-phosphonopentanoic acid; DNQX, 6,7-dinitroquinoxaline-2,3-dione; EE, enriched environment; EPSC, excitatory postsynaptic current; Hepes, *N*-(2-hydroxyethyl)piperazine-*N*′-(2-ethanesulfonic acid); HF, high-frequency; I_{AMPA}, AMPA current; I_{NMDA}, *N*-methyl-D-aspartate current; IPI, interpulse interval; IPSC, inhibitory postsynaptic current; LF, low-frequency; mEPSC, miniature excitatory postsynaptic current; NMDA, *N*-methyl-D-aspartate; NMDAR, *N*-methyl-D-aspartate receptor; PPR, paired pulse ratio; QX314, lidocaine *N*-ethyl bromide.

The anatomic connectivity and physiological properties of the CNS are determined by a combination of genetic programs and by the type and amount of sensory input (Bartoletti et al., 2004). Many studies have shown anatomical and cellular consequences of the exposure to a sensory enriched environment (EE, Diamond et al., 1964; Volkmar and Greenough, 1972).

While several studies reported the effects of EE on synaptic transmission in the hippocampus (Duffy et al., 2001; Artola et al., 2006; Irvine and Abraham, 2005; Foster and Dumas, 2001), scant information is available on the effects of EE on the synaptic properties of the neocortex. In a previously developed model of auditory EE, Engineer et al. (2004) demonstrated large increases in surface auditory evoked potentials (AEPs) and in the number of action potentials recorded at the auditory cortex. EE also increased the degree of auditory gating (paired pulse depression) recorded with both epidural and intracortical electrodes (Percaccio et al., 2005). Physiological differences detected in the auditory cortical responses might originate in the cortex itself, or might rather be the result of a different subcortical processing between control and EE animals. The purpose of this study was to identify a possible local, cortical source of differential processing between control and EE animals. We used the same behavioral paradigm of auditory EE reported above (Engineer et al., 2004; Percaccio et al., 2005) to investigate differences in pharmacologically isolated excitatory and inhibitory synapses in EE vs. control-raised animals in the auditory cortex of the rat.

EXPERIMENTAL PROCEDURES

Environmental conditions

Twenty-three control and 27 EE-raised Sprague–Dawley rats were used in this study. All rats were housed with their mothers and littermates until they reached an age of 21 days. They were then randomly separated and placed into either enriched or standard housing conditions. Rats were given a code of colored tail stripes in order to preserve their housing condition's confidentiality from experimenters and avoid any unintentional bias. All rats were provided with food and water *ad libitum*. A reverse 12-h light/dark cycle and constant humidity and temperature were maintained for both groups. All experimental procedures were performed in accordance with the NIH Ethical Treatment of Animals and were approved by the University Committee on Animal Research at the University of Texas at Dallas. The number of animals was kept to the minimum necessary to ensure statistical validity. The enriched environment did not induce any pain to the experimental animals, nor did the anesthesia before decapitation. Housing conditions were nearly identical to those described in previous studies (Per-

0306-4522/07$30.00+0.00
doi:10.1016/j.neuroscience.2006.12.061

caccio et al., 2005; Engineer et al., 2004). The EE exposure time for this study was 5–6 weeks.

Four to eight rats were housed together in the EE cage which was located in a separate room from the main rat colony at UTD. This cage (76×45×90 cm) had four levels accessible by ramps. The environment's complexity was augmented by bells, wind chimes, and chains. Tones at 2.1 or 4.0 kHz were sounded when touch plates (located at the bottom of two of the ramps) were depressed. Additionally a chime was sounded when an infrared beam was broken in front of the water source and each rotation of an exercise wheel activated a small green light emitting diode and a 3 kHz tone. These devices were designed and positioned in such a way that their sounds provided information about movement in a specific location within the cage at a particular time.

Other meaningful sounds were provided by a CD player. Every 2–60 s, a randomly selected sound was played, including simple tones, amplitude and frequency modulated tones, noise bursts, and other complex sounds (rat vocalizations, classical music, rustling leaves, etc.). Seven of the 74 sounds activated a pellet dispenser (Med Associates, St. Albans, VT, USA) that delivered a sugary treat intended to encourage attention to the sounds. The rewarded tracks included interleaved tones of different carrier frequencies (25 ms long and 4, 5, 9, 12, 14, and 19 kHz tones with inter-stimulus intervals ranging from 50 ms to 2 s) and frequency modulated sweeps (one octave up or down in a 140 or 300 ms sweep with inter-stimulus intervals ranging from 80 to 800 ms). All sounds were <75 dB SPL, provided 24 h a day and spanned the entire hearing range of the rat (1–45 kHz).

Standard environment cages were 26×18×18 cm and included one to two rats per cage. The standard housing environment exposed rats to vocalizations from 20–30 other rats housed in the same room, in addition to general sounds (which were also heard by rats in the EE) resulting from daily traffic, cleaning, and feeding while they were most active. Although rats housed in both environments heard approximately the same number of sounds each day, sounds in the EE condition were more diverse, and provided more behaviorally significant information than the sounds in the standard condition.

Slice preparation

We followed an auditory cortex slice preparation protocol similar to one previously described (Atzori et al., 2001). After exposure to enriched or standard environmental conditions (as described above), 6- to 9-week-old Sprague–Dawley rats were anesthetized (evaluated by toe-pinch response) in a chamber with vaporized isoflurane (0.2 ml/100 g) and immediately decapitated. The brains were carefully extracted and immersed in a solution (slicing artificial cerebrospinal fluid (ACSF)) chilled to approximately 0.5 °C containing (mM) 130 NaCl, 3.5 KCl, 10 glucose, 24 $NaHCO_3$, 1.25 NaH_2PO_4, 0.5 $CaCl_2$ and 1.5 $MgCl_2$, and saturated with a mixture of 95% O_2 and 5% CO_2 (pH ≈7.35 osmolarity 301±5 mOsm). The low concentration of calcium decreases the spontaneous release of glutamate prolonging viability of the preparation. After removal of the cerebellum, a vibratome (VT1000, Leica, Wetzlar, Germany) was used to cut 270 μm-thick coronal slices from the first sixth of the caudal part of the brain, corresponding to the primary auditory area (A1). Slices were then placed into an incubating chamber super-fused with the ACSF solution described above and incubated at 33 °C for approximately 1 h, and then maintained at room temperature until used for recording.

Electrophysiology

Slices were transferred to a recording chamber and immersed in a solution (recording-ACSF) similar to the slicing-ACSF solution described above containing 1.5 mM $CaCl_2$ rather than 0.5 mM. Pyramidal neuron selection procedures were adopted from those described previously (Atzori et al., 2005). Cells with an obvious apical dendrite located in layer II/III or V and dorsal to the ectosylvian region were visually selected using a Luigs and Neumann 380 FM Workstation (Luigs & Neumann, Ratingen, Germany) with Olympus BX51 WI optics and an infrared camera system (Olympus, Tokyo, Japan).

Perforated patch clamp recordings were performed using techniques similar to the whole cell patch clamp technique already described (Atzori et al., 2001), with an internal recording solution containing, in addition, the antibiotic amphotericin B (3.24 mM). Intracellular recording solution contained in mM 100 CsCl, 5 1,2-bis(2-aminophenoxy)ethane-*N*,*N*,*N*′,*N*′-tetraacetic acid K (BAPTA-K), 1 lidocaine *N*-ethyl bromide (QX314), 1 $MgCl_2$, 10 Hepes, 4 glutathione, 1.5 $ATPMg_2$, 0.3 GTPNa2, 8 biocytin (pH ≈7.35 osmolarity 270±10 mOsm). Amphotericin B was used to form pores in the neuronal membrane layer allowing electrical access (perforated-patch) without the intracellular dialysis normally associated with whole cell patch clamping. The pulled glass electrode tips (5–8 MΩ) were backfilled with the intracellular recording solution after the most distal 200 μm were filled with the amphotericin B free intracellular solution in order to prevent tip clogging during electrode-membrane seal formation. Holding current and input resistance (Ω_{in}) were continuously monitored with a 2 mV negative pulse delivered before the paired pulse protocols. Recording was delayed until the voltage-gated sodium channel blocker lidocaine (QX314) reached an intracellular concentration high enough to prevent action potentials and input resistance stabilized (15–20 min).

Electrically evoked postsynaptic currents were measured by delivering two electric stimuli (90–180 μs) either 20, 40, 50, 100, 500, or 1000 ms apart every 8 s, in the order stated, with a stimulus isolator (A365 triggered by a DS8000-82112 Digital Simulator, both from World Precision Instruments, Sarasota, FL, USA) through a glass stimulation mono-polar electrode filled with recording-ACSF, and always placed at the same distance (approximately 120 μm) from the recording electrode, and averaged over 4 to 10 responses. The intensity of the stimulation was standardized as the one determining a postsynaptic response corresponding to 80% of the maximal response.

Excitatory postsynaptic currents (EPSCs) were measured in a bath of bicuculline (10 μM) at a holding potential of −60 mV for inward currents and +60 mV for outward currents and reversibly blocked by DNXQ (10 mM) and kynurenic acid (2 mM) indicating a glutamatergic composition. EPSC's amplitude was measured at the peak of inward current as AMPA current (I_{AMPA}), and current amplitude 45 ms after the outward excitatory current peak was taken as the estimate of *N*-methyl-D-aspartate (NMDA) current (I_{NMDA}). Similar methods were previously described (Duffy et al., 2001). We selected the ratio between *N*-methyl-D-aspartate receptor (NMDAR)-mediated currents and AMPA receptor (AMPAR)-mediated currents (I_{NMDA}/I_{AMPA}) as an indicator of postsynaptic function. Paired pulse ratio (PPR) was defined as the ratio between the mean of the peak of the second inward current response and the mean of the peak of the first inward current response (P_2/P_1).

Inhibitory postsynaptic currents (IPSCs) were measured at a holding potential $V_h = -60$ mV in a bath solution containing 10 μM 6,7-dinitroquinoxaline-2,3-dione (DNQX) and 2 mM kynurenic acid for blocking glutamate receptor-mediated currents. The intracellular recording solution provided a reversal potential for Cl^- of approximately 0 mV. IPSCs were blocked by bicuculline (10 μM), indicative of their GABAergic origin.

Signals were acquired via a Digidata 1322A 16 bit data acquisition system controlled by Clampex 9.2 and Multiclamp 700B software (Axon Instr., Foster City, CA, USA) and filtered at 3200 Hz (low pass) with a Frequency Devices 900 tunable active filter (Frequency Devices, Haverhill, MA, USA). The recording chamber was situated within a 1 m^3 Faraday cage on an anti-vibration table (Technical Manufacturing Corporation, Peabody,

MA, USA) attached to a dedicated ground. DNQX and amphotericin B were dissolved in dimethylsulphoxide (DMSO). All other drugs were dissolved in de-ionized H_2O. All drugs in this study were purchased from Sigma (St. Louis, MO, USA) or from Tocris (Ellisville, MO, USA).

Data analysis

Statistical analysis was performed with Clampfit 9.2, SigmaPlot 8.0, and Microsoft Excel software. A Student's unpaired *t*-test was used for comparison between different groups of cells. Data were reported as significantly different only if $P<0.05$.

Neural model

We used MatLab to develop a realistic neural network model for simulating the effects of EE on cortical processing. The model, described in more detail in the appendix, used a three-compartment pyramidal neuron and a single compartment interneuron with previously described voltage-gated conductances (Wang, 1998). Synaptic release elicits α-function like synaptic currents (see the Results and Appendix sections). We adapted the parameters of a series of neocortical models of synaptic release reported previously (Brunel and Wang, 2001; Tiesinga and Sejnowski, 2001; Varela et al., 1997) to reproduce the paired pulse data measured in the present study.

RESULTS

AMPAR-mediated currents in layer II/III

Since EE increases 3H AMPA binding in the hippocampus (Foster et al., 1996) and has been suggested to enhance glutamatergic activity (Foster and Dumas, 2001), we first measured the amplitude of electrically evoked EPSCs in visually identified neurons from layer II/III of the auditory cortex. A paired pulse protocol was applied with an interpulse delay varying between 20 and 1000 ms, for evaluating possible presynaptic differences between EE and the control group. In order to avoid a possible bias due to different stimulation conditions, the distance between stimulation and recording electrode and the stimulation intensity were kept in a narrow range. All recordings were performed with the experimenter unaware of each rat's housing condition. No significant changes in input resistance (271 ± 24 MΩ in control, $n=12$, vs. 234 ± 28 MΩ in EE, $n=13$) were evident between control and EE. The mean stimulation intensity was also similar between groups (3.91 ± 0.53 μA in control vs. 3.75 ± 0.32 μA in EE). In these conditions, the amplitude of AMPAR-mediated current (I_{AMPA}) from EE animals was much larger in EE,

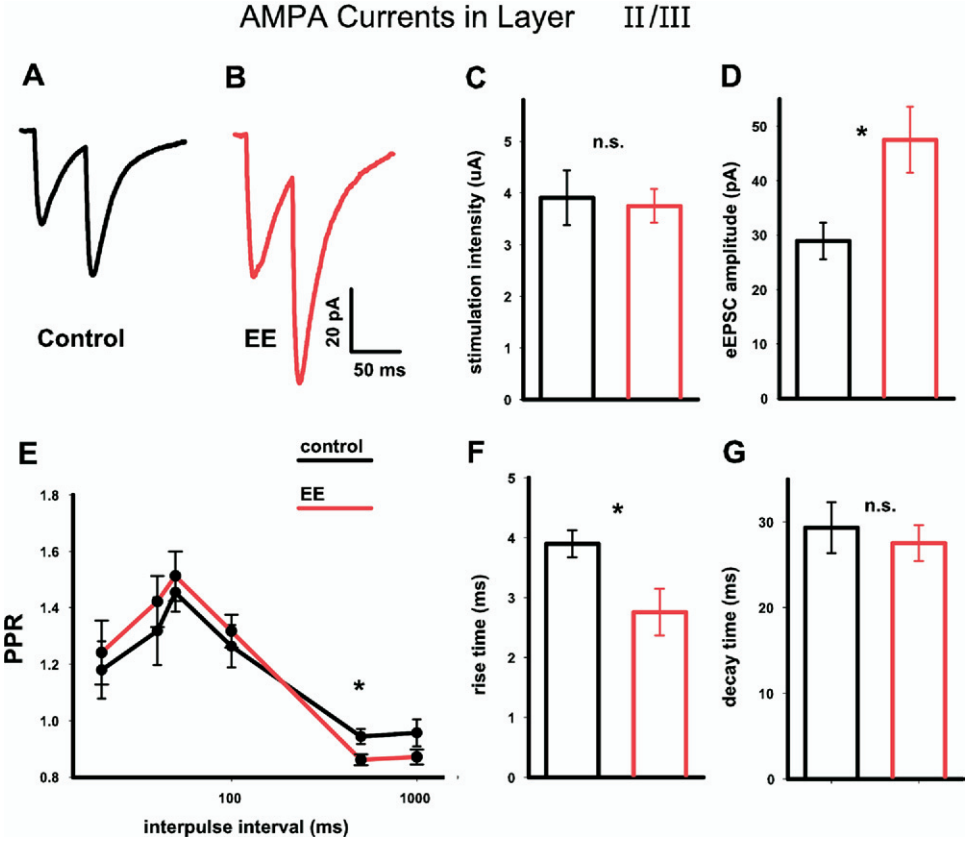

Fig. 1. AMPAR-mediated currents in layer II/III. (A, B) Mean traces for control ($n=10$) and EE ($n=11$) animals. (C) Intensity of the electrical stimulation for control (red) and EE (black) did not change. (D) Mean of the peak amplitude of the AMPAR-mediated current in control (black, $n=10$) vs. EE (red, $n=11$). The mean amplitude was more than 60% larger in EE animals. (E) PPR ($PPR=A_2/A_1$). PPR at an IPI of 500 ms was smaller in EE animals (0.943 ± 0.026 in control vs. 0.877 ± 0.018 in EE, $n=10$ control; $n=11$ in EE). (F) Rise time and (G) decay time of the evoked EPSC. The rise time is shorter in EE animals while no differences are present in the decay time. Altogether, these data suggest that EE elicits changes in glutamatergic synaptic signals. For interpretation of the references to color in this figure legend, the reader is referred to the Web version of this article.

compared with controls (I_{AMPA}(EE)/I_{AMPA}(control)=164±12%) (n=10 in control and 11 in EE, representative traces in Fig. 1A and B), suggesting that EE strongly enhances excitatory currents. Fig. 1C and D report the mean evoked EPSCs in control vs. EE animals and the mean of the stimulation intensity in the two conditions. PPR, calculated as the ratio between the second and the first responses (A_2/A_1) was measured at a series of interpulse intervals (IPIs) in the range 20–1000 ms. EE animals had a lower PPR for IPI=500 ms ($P<0.05$, n=10 ctr, n=11 EE, Fig. 1E), while no differences were detected for other IPIs. We also measured evoked EPSC kinetics, finding that rise time in EE was 29±6% shorter with respect to control, while no difference was detected in the decay time (Fig. 1F and G respectively).

Altogether, these data suggest that EE alters glutamatergic synaptic responses in layer II/III.

Miniature excitatory postsynaptic currents (mEPSCs)

In order to gain a deeper understanding of the nature and origin of the difference between control and EE glutamatergic synapses we measured the characteristics of spontaneous release of glutamate measured in the presence of the sodium channel blocker tetrodotoxin (TTX, 0.5 μM), and the $GABA_A$ channel blocker bicuculline 10 μM, or picrotoxin (100 μM) from layer II/III neurons.

A first round of analysis showed no differences in the frequency of the mEPSC, in spite of a marked tendency for an increased ($f_{control}$=0.20±0.10 Hz, n=8, vs. fEE=0.99±0.57, n=10, n.s.), and a decrease in the mEPSC amplitude ($A_{control}$=12.7±1.7 pA, vs. 8.7±0.9 pA, same sample). An analysis of the factors contributing to the large variability within the whole sample indicated the existence of two separate cell populations receiving respectively a high-frequency (HF; below 0.15 Hz, mean 0.072±0.012 Hz) and a low-frequency (LF; above 0.45 Hz, mean 1.53±0.75 Hz) mEPSC input. The mEPSC amplitude of the two populations did not differ ($A_{control}$=9.8±1.5 pA vs. AEE=11.5±1.2 pA, n.s.). The difference between control and EE mEPSC was observed in the proportion of HF- vs. LF-receiving neurons ($HF/LF_{control}$=0.33, 2 of 6, vs. HF/LF_{EE}=1.00, 5 of 5).

GABAergic currents in layer II/III

The changes in extracellular signals associated with EE (Percaccio et al., 2005) might be due to an increase in excitatory drive and/or decreased inhibition. Decreased inhibition might be a consequence of a decrease in $GABA_A$ receptor-mediated currents. We tested the hypothesis of a decrease in synaptic inhibition by directly measuring GABAergic currents (eIPSCs) from layer II/III neurons using a protocol of stimulation similar to the one described in the previous paragraph, but in the presence of the glutamate ionotropic receptor blockers DNQX (10 μM) and kynurenic acid (2 mM). The remaining currents were blocked by 10 μM bicuculline, confirming their GABAergic nature.

Evoked IPSCs amplitude was not different in control vs. EE animals (Fig. 2A, n=8). No difference in rise- or decay-time was detected (Fig. 2B and C, same sample as Fig. 2A). The same pair pulse protocol used for AMPAR-mediated currents (IPIs in the range 20–1000 ms) was used to measure possible changes in PPR (Fig. 2D, same sample as above). PPR too remained unchanged between the two conditions ($P>0.5$, n=8 each). These data suggest that changes in inhibition are not likely to play a major role in EE.

AMPA-mediated currents in layer V

The change in the AMPAR-mediated signals might be a selective, layer-specific change in synaptic strength, or might rather be associated with a generalized increase in synaptic function throughout the cortical mantle. For determining the specificity of the synaptic increase, we used the same protocol described previously for measuring the properties of AMPAR-mediated currents in layer V of the auditory cortex.

We could not detect any differences in synaptic strength, kinetic properties or PPR in ePSCSs recorded from layer V of the auditory cortex (n=5 in control; n=8 in EE). The results are displayed in Fig. 2E, F, G and H.

Collectively, these results indicate that the increase in AMPAR-mediated results detected in layer II/III, is synapse specific and layer specific.

I_{NMDA}/I_{AMPA}

Recent evidence highlighted that different types of glutamatergic synapses undergo a maturation process consisting in the activity-dependent insertion of AMPARs in a postsynaptic membrane initially containing only or prevalently NMDARs (reviewed in Isaac et al., 1999). We considered the hypothesis that EE would increase I_{AMPA} using a similar mechanism. To test this hypothesis we measured I_{AMPA} as well as NMDAR-mediated currents (I_{NMDA}) at the same synaptic connection, by first measuring I_{AMPA}, holding the membrane potential at V_m=−60 mV, and subsequently measuring I_{NMDA}, upon changing V_m to +60 mV, in order to get rid of the Mg^{2+} block. An estimate of the ratio I_{NMDA}/I_{AMPA} was obtained by dividing the current measured at V_h=+60 mV (45 ms after the stimulus artifact, to minimize the contribution of AMPAR-mediated currents), by the peak amplitude of the I_{AMPA} (see Experimental Procedures). No change was detected in the ratio I_{NMDA}/I_{AMPA}, indicating that changes in I_{AMPA} were accompanied by a proportional increase in I_{NMDA} (n=6, control; n=8 EE). A representative trace is shown in Fig. 3A. Fig. 3B shows the mean of the ratio I_{NMDA}/I_{AMPA}.

We also measured I_{NMDA}/I_{AMPA} by pharmacologically isolating I_{AMPA} after application of the I_{NMDA} blocker D-2-amino-5-phosphonopentanoic acid (APV, 100 μM). I_{NMDA}/I_{AMPA} did not differ with this method either ($I_{NMDA}/I_{AMPA\ control}$=0.93±0.06, n=5, vs. $I_{NMDA}/I_{AMPA\ EE}$=1.14±0.36 in EE, n=6, n.s.).

Neuronal models of the effects of EE

We built a realistic neuronal model of pyramidal cell and GABAergic interneuron, based on a set of conductances

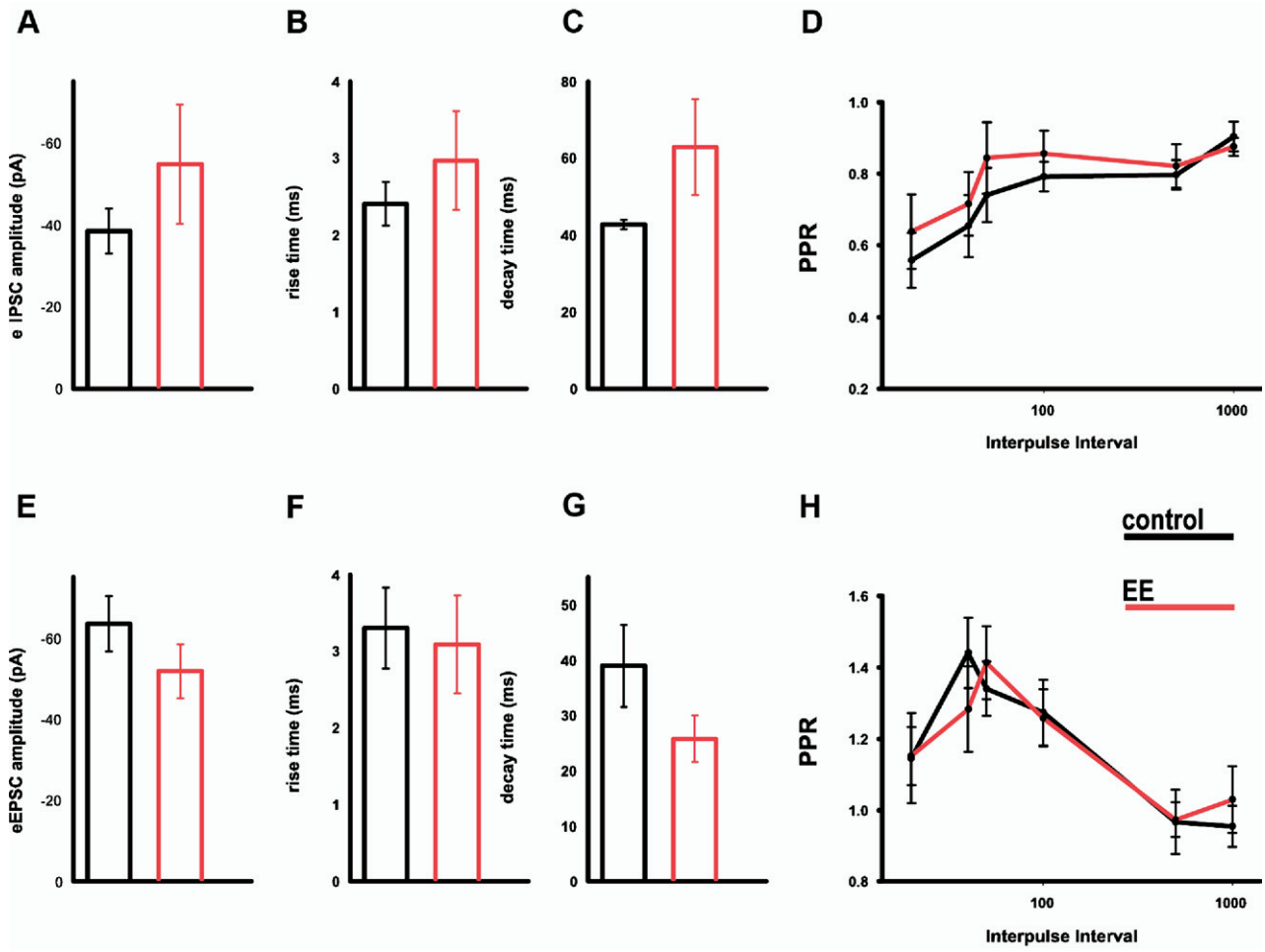

Fig. 2. Neurotransmitter- and layer-specificity of the synaptic changes. (A–D) Amplitude, rise time, decay time and PPR of GABAergic currents in layer II/III do not differ in control or in EE (n=8 each). (E–H) Amplitude, rise time, decay time and PPR in AMPAR-mediated glutamatergic currents of layer V do not differ between control and EE (n=5 control; n=8 EE).

present in the two type of cells, discussed in more detail in the Experimental Procedures section and in the Appendix, and used them to construct two minimal neural networks, modeling some possible consequences of the synaptic

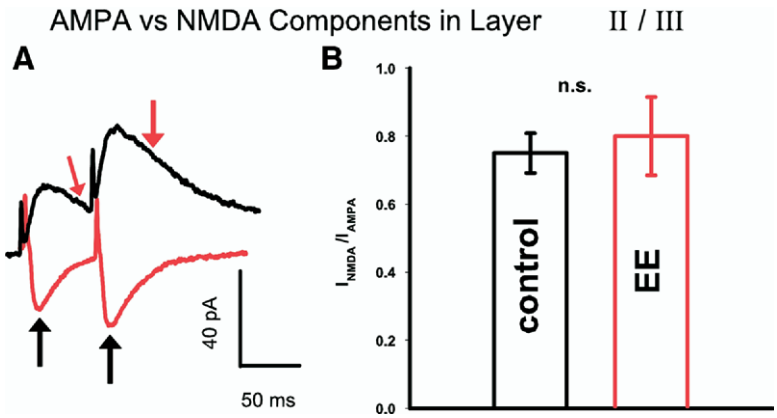

Fig. 3. Invariance of the I_{NMDA}/I_{AMPA}. (A) The AMPAR- and the NMDAR-dependent components of the glutamatergic currents were measured by recording a synaptic current at a holding voltage. V_h=−60 mV or V_h=+60 mV, the latter one to eliminate Mg^{2+} block. I_{AMPA}s were measured, as elsewhere in the study, at the peak, NMDA currents were measured 45 ms after stimulation (arrow), to minimize any contamination by the AMPA component. (B) Mean I_{NMDA}/I_{AMPA} in control (black, n=6) vs. EE animals (red, n=8). The parallel change in I_{NMDA} and I_{AMPA} supports the idea that EE induces a global increase in excitatory synaptic function. For interpretation of the references to color in this figure legend, the reader is referred to the Web version of this article.

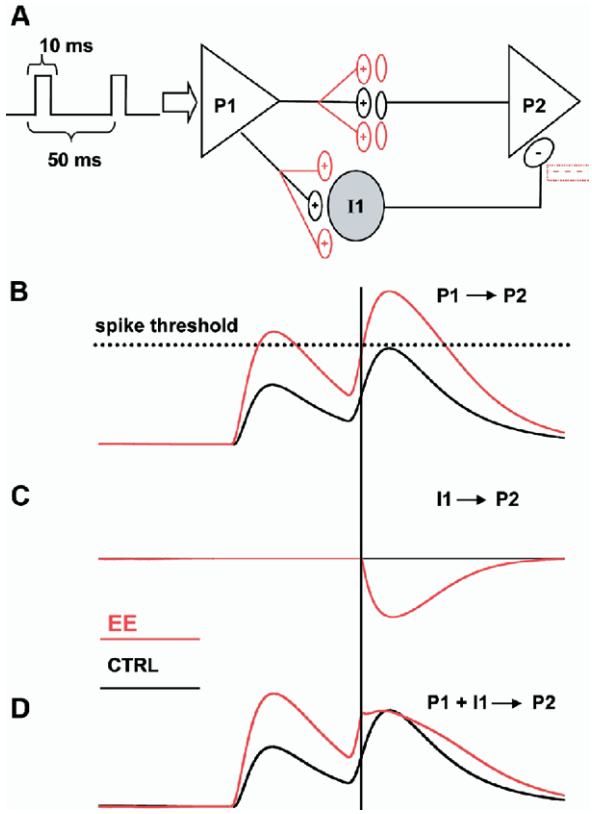

Fig. 4. Model of EE and enhanced gating. A simplistic model of cortical synaptic circuit with an input layer (P1), and output layer (P2) and an inhibitory interneuron (I1). Each model neuron represents a population of independent synaptic units. P1 receives two square current injections (10 ms–100 ms between pulses) generating one action potential each. In the control situation none of the two synaptic responses generate an action potential in I1 (B, C, black line). In the EE only the second response generates an action potential in I1 (B and C, red lines), contributing to the decrease in PPR (D). For interpretation of the references to color in this figure legend, the reader is referred to the Web version of this article.

changes induced by EE. Both instances of the simulations presented in the following two paragraphs compared the function of a small circuit in control or with increased excitatory synaptic strength as observed in EE.

Increase in auditory gating. The model represented in Fig. 4A illustrates a network of two pyramidal (P) cells connected in series, plus a feed-forward GABAergic interneuron (I) connecting the input layer neuron (P1) with the output layer neuron (P2). Every synapse can be regarded as a large number of independent identical synapses impinging upon the same cellular target. We simulated the response of the network to two small square current pulses (10 ms) delivered at 100 ms interpulse delay, evoking one spike each in P1. In a particular set of cells, in the control situation, the two spikes induce a couple of facilitating, subthreshold synaptic responses both in P1 and I1 (Fig. 4B and C, black traces). The resultant synaptic signal in P2 is not affected by the presence of I1 (Fig. 4D, black trace). In EE, because of the increase in excitatory synaptic strength and due to the facilitation at the glutamatergic synapse, a firing threshold is reached by I1, which fires at the second stimulus, resulting in the decrease of the second, but not the first synaptic signal detected in P2 (Fig. 4B, C, and D). The short delay associated with axo-somatic inhibition vs. axo-dendritic excitation contributes to minimize the time difference between the signal transiting in the disynaptic (P1–I1–P2) or the monosynaptic (P1–P2) branches, increasing the contribution of inhibition to PPR.

In the real situation the signal is determined by the summation of the excitatory plus the inhibitory synaptic currents, which includes an unknown statistical distribution of firing and nonfiring interneurons. A reasonable possibility is that such distribution elicits a modest PPR in control, substituted by a larger PPR in EE.

Enhanced robustness to input phase differences. One important property of auditory neurons is the capability to integrate oscillatory inputs with slight phase differences. We tested the hypothesis that auditory EE modifies the dependence of cell firing on input phase differences by using a neuronal network with two independent pyramidal neurons in the input layer (P1 and P2, Fig. 5A), and one pyramidal neuron in the output layer (P3). Two sinusoidal inputs at the same frequency with different phase are fed into P1 and P2 respectively (Fig. 5A). The amplitude of the sinusoidal was selected as to generate a minimal firing in the postsynaptic neuron (one or two spikes), while the sum of the two inputs in phase generated a higher but still non-saturated postsynaptic firing. We simulated the response of the system for three input frequencies (5, 20 and 50 Hz), in control or in EE (Fig. 5B, C and D).

As expected, the model showed that EE increases the mean firing frequency at all tested frequencies (Fig. 5B, C and D).

At all frequencies a non-zero phase difference (10–80°) maximizes the firing frequency due to the increased interval for synaptic summation (Fig. 5B, C, D). Remarkably, at all the simulated input frequencies, EE greatly increased the width of the phase interval at which the output firing frequency was maximal. At intermediate frequencies (20 Hz, Fig. 5C) the optimal phase difference was enlarged by almost 90°. These results suggest not only that the simultaneity of the input signals is not necessary for maximizing the firing frequency, but also that the presence of a phase difference between two input signals can increase the output firing probability. EE synapses increase excitability not with a homogeneous upward shift of the firing frequency but rather by increasing the width of the phase-dependence firing profiles as summarized in Table 1.

DISCUSSION

The influence of the environment on animal behavior has long been documented. Several anatomical and physiological studies have clearly demonstrated an involvement of the hippocampus and related structures (Green and Greenough, 1986; Foster et al., 2000; Sharp et al., 1985; Faherty et al., 2003; Foster and Dumas, 2001). Recently more attention has been focused on how EE affects other

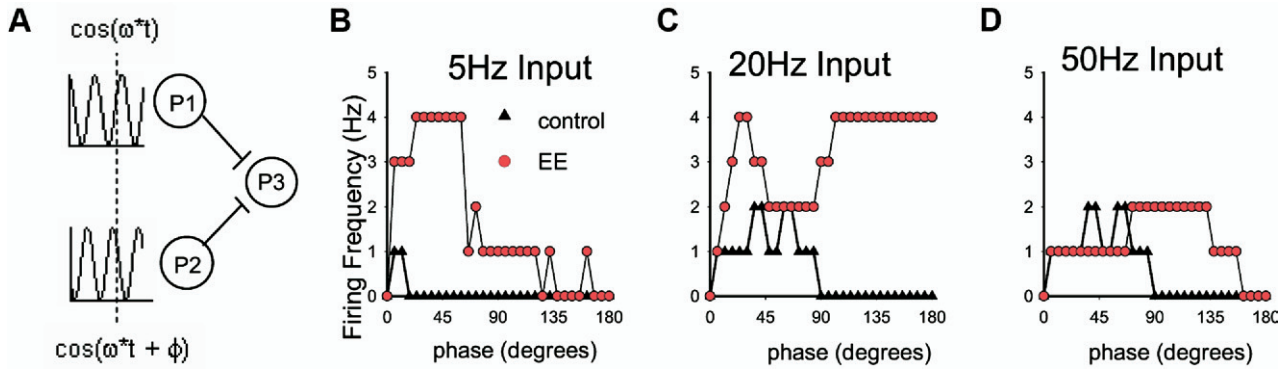

Fig. 5. Enhanced robustness of EE synaptic summation. (A) A second neural model simulated the effect of EE on the response to two oscillatory inputs, each separately below threshold. P3 is the output layer receiving input from two pyramidal cells receiving a subthreshold sinusoidal wave at the same frequency but with different phase. (B–D) Firing frequency variation in P3 for control (black line) or EE (red line) at the input frequencies of 5, 20, or 50 Hz, as a function of the phase difference between the two inputs. At all frequencies a slight phase difference (≅20°) elicits an increase in the response due to the longer interval for synaptic integration. At all input frequencies, the output firing frequency is maximal within a certain phase interval whose width varies from 20° (B) to 80° (C and D). Environmental enrichment widens this interval up to threefold. For interpretation of the references to color in this figure legend, the reader is referred to the Web version of this article.

brain areas, including the neocortex (Nithianantharajah et al., 2004). In particular, large anatomical rearrangements of dendritic processing have been documented in the parietal cortex (Leggio et al., 2005), prefrontal cortex (Dierssen et al., 2003) as well as in monoaminergic neocortical innervation (Zhu et al., 2005; Hellemans et al., 2005). In the cat primary visual cortex, EE has been found to be effective in rescuing ocular dominance columns impaired by dark rearing (Bartoletti et al., 2004). In the primary auditory cortex, EE induces major physiological rearrangements, detected as changes in single cell response properties as well as in scalp recording (Engineer et al., 2004; Percaccio et al., 2005).

Our results showed a strong and selective increase in amplitude and a change in kinetics of glutamatergic responses. These data are in agreement with the general increase in the excitability, firing rate and decrease in latency in the AEP amplitude observed in the response to short (25 ms) tones *in vivo* (Engineer et al., 2004).

The stability of the ratio between NMDAR-mediated and AMPAR-mediated currents indicates that EE is not associated with a selective insertion of new AMPARs in the postsynaptic membrane ("silent" synapse "awakening"). Yet, other postsynaptic changes preserving I_{AMPA}/I_{NMDA} might take place at EE synapses.

The dramatic increase in EPSC amplitude might simply reflect an increase in the total number of excitatory spines, in agreement with previous findings (Dierssen et al., 2003). Similarly, the lack of changes in evoked EPSC PPR at short (<500 ms) IPIs does not allow exclusion of the presence of presynaptic rearrangements preserving PPR. This interpretation is corroborated by the observation of a larger number of cells receiving HF mEPSC, suggesting an increase in either the number of presynaptic fibers projecting to a subset of neurons, or in the capability of releasing neurotransmitter in a subset of presynaptic fibers.

Table 1. Width of the total phase interval inducing maximal output firing

Treatment	Stimulation frequency		
	5 Hz	20 Hz	50 Hz
Control (CE)	20°	80°	80°
EE	60°	150°	140°
Absolute increase	40°	70°	60°

Values indicate width of the half-maximal frequency profile. EE widens two- to threefold the width of the phase interval inducing maximal firing, corresponding to a more robust processing filter.

The lack of changes in inhibitory responses does not support a major role for inhibition in the EE-driven re-shaping of auditory cortical responses. A sharp-electrode study on hippocampal non-pharmacologically dissected synaptic currents reported a similar conclusion (Foster and Dumas, 2001), although the invariance of inhibitory responses might be a reflection of the heterogeneity of cortical interneuronal types.

The increase in synaptic efficacy could be the result of a generalized synaptic strengthening or could be a layer-specific phenomenon. The unchanged excitatory responses from layer V would suggest the second hypothesis, indicating layer II/III as a privileged substrate for the solidification of cortical plasticity. A similar conclusion was previously reached with an anatomical–morphological study (Johansson and Belichenko, 2002), and is expected if EE is caused by spike-time-dependent plasticity, since the threshold for action potentials in layer V is approximately 10 mV more positive than in layer II/III (Atzori et al., 2004).

The increase in synaptic amplitude after exposure to the EE might derive from the transformation of low-probability and small amplitude synapses into high probability, large amplitude synapses (Atzori et al., 2001). Yet, high probability synapses possess slower rise times and smaller PPR with respect to low-probability synapses, contrasting with our current finding that EE decreases rise-time and leaves PPR unchanged, suggesting a different origin for the synaptic changes in EE.

The use of a computational model corroborated the hypothesis that the increase in auditory gating in EE (Percaccio

et al., 2005) is due in part or completely to local, cortico-cortical changes in excitatory synaptic strength.

Auditory information is largely conveyed by low frequency envelope signals surfacing onto AI with slight phase differences within an isofrequency contour. Our computational model showed that the synaptic changes associated with the EE not only produce an expectable increase in firing rate but that they also decrease the dependence of the postsynaptic firing rate on the input phase differences, in the case of two slow frequency de-phased inputs. In fact, at all studied input frequencies, the increase in firing rate corresponding to a small phase increase displayed in control is replaced in EE by a solid enhancement almost independent on the phase difference between the two inputs, making synaptic summation more robust in EE.

Although our data indicate that EE causes significant cortical plasticity, we cannot exclude the possibility that noncortical auditory relays are also modified by EE, introducing a further component to the EE-induced alteration of the cortical signal detected by AEP (Percaccio et al., 2005). In conclusion, we demonstrated for the first time that EE induces a change in the efficacy of glutamatergic synapses within the primary auditory cortex, associated with a major postsynaptic rearrangement compatible with an increase in the total number of synaptic connections.

Acknowledgments—J.A.N. performed most of the patch-clamp experiments, analyzed and elaborated data and figures, and contributed to writing the final version of the manuscript, V.P.J. raised the EE animals and contributed to the discussion, H.S. recorded part of the mEPSC and of the APV experiments, L.D. wrote and ran the MatLab program using literature and original data, M.P.K. contributed to the original idea, to the design of the experiments and to the final version of the manuscript, M.A. contributed to the original idea and to the design of the experiments, and wrote the final version of the manuscript. Grants: NIDCD 1R01-DC005986-01A1 and NARSAD foundation/Sidney Baer Trust (M.A.) and American Academy of Audiology to J.A.N.

REFERENCES

Artola A, von Frijtag JC, Fermont PC, Gispen WH, Schrama LH, Kamal A, Spruijt BM (2006) Long-lasting modulation of the induction of LTD and LTP in rat hippocampal CA1 by behavioural stress and environmental enrichment. Eur J Neurosci 23:261–272.

Atzori M, Flores HJ, Pineda JC (2004) Interlaminar differences of spike activation threshold in the auditory cortex of the rat. Hear Res 189:101–106.

Atzori M, Kanold PO, Pineda JC, Flores-Hernandez J, Paz RD (2005) Dopamine prevents muscarinic-induced decrease of glutamate release in the auditory cortex. Neuroscience 134:1153–1165.

Atzori M, Lei S, Evans DI, Kanold PO, Phillips-Tansey E, McIntyre O, McBain CJ (2001) Differential synaptic processing separates stationary from transient inputs to the auditory cortex. Nat Neurosci 4:1230–1237.

Bartoletti A, Medini P, Berardi N, Maffei L (2004) Environmental enrichment prevents effects of dark-rearing in the rat visual cortex. Nat Neurosci 7:215–216.

Brunel N, Wang XJ (2001) Effects of neuromodulation in a cortical network model of object working memory dominated by recurrent inhibition. J Comput Neurosci 11:63–85.

Diamond MC, Krech D, Rosenzweig MR (1964) The effects of an enriched environment on the histology of the rat cerebral cortex. J Comp Neurol 123:111–120.

Dierssen M, Avides-Piccione R, Martinez-Cue C, Estivill X, Florez J, Elston GN, DeFelipe J (2003) Alterations of neocortical pyramidal cell phenotype in the Ts65Dn mouse model of Down syndrome: effects of environmental enrichment. Cereb Cortex 13:758–764.

Duffy SN, Craddock KJ, Abel T, Nguyen PV (2001) Environmental enrichment modifies the PKA-dependence of hippocampal LTP and improves hippocampus-dependent memory. Learn Mem 8:26–34.

Engineer ND, Percaccio CR, Pandya PK, Moucha R, Rathbun DL, Kilgard MP (2004) Environmental enrichment improves response strength, threshold, selectivity, and latency of auditory cortex neurons. J Neurophysiol 92:73–82.

Faherty CJ, Kerley D, Smeyne RJ (2003) A Golgi-Cox morphological analysis of neuronal changes induced by environmental enrichment. Brain Res Dev Brain Res 141:55–61.

Foster TC, Dumas TC (2001) Mechanism for increased hippocampal synaptic strength following differential experience. J Neurophysiol 85:1377–1383.

Foster TC, Fugger HN, Cunningham SG (2000) Receptor blockade reveals a correspondence between hippocampal-dependent behavior and experience-dependent synaptic enhancement. Brain Res 871:39–43.

Foster TC, Gagne J, Massicotte G (1996) Mechanism of altered synaptic strength due to experience: relation to long-term potentiation. Brain Res 736:243–250.

Green EJ, Greenough WT (1986) Altered synaptic transmission in dentate gyrus of rats reared in complex environments: evidence from hippocampal slices maintained in vitro. J Neurophysiol 55:739–750.

Hellemans KG, Nobrega JN, Olmstead MC (2005) Early environmental experience alters baseline and ethanol-induced cognitive impulsivity: relationship to forebrain 5-HT1A receptor binding. Behav Brain Res 159:207–220.

Irvine GI, Abraham WC (2005) Enriched environment exposure alters the input-output dynamics of synaptic transmission in area CA1 of freely moving rats. Neurosci Lett 391:32–37.

Isaac JT, Nicoll RA, Malenka RC (1999) Silent glutamatergic synapses in the mammalian brain. Can J Physiol Pharmacol 77:735–737.

Johansson BB, Belichenko PV (2002) Neuronal plasticity and dendritic spines: effect of environmental enrichment on intact and postischemic rat brain. J Cereb Blood Flow Metab 22:89–96.

Leggio MG, Mandolesi L, Federico F, Spirito F, Ricci B, Gelfo F, Petrosini L (2005) Environmental enrichment promotes improved spatial abilities and enhanced dendritic growth in the rat. Behav Brain Res 163:78–90.

Nithianantharajah J, Levis H, Murphy M (2004) Environmental enrichment results in cortical and subcortical changes in levels of synaptophysin and PSD-95 proteins. Neurobiol Learn Mem 81:200–210.

Percaccio CR, Engineer ND, Pruette AL, Pandya PK, Moucha R, Rathbun DL, Kilgard MP (2005) Environmental enrichment increases paired-pulse depression in rat auditory cortex. J Neurophysiol 94:3590–3600.

Sharp PE, McNaughton BL, Barnes CA (1985) Enhancement of hippocampal field potentials in rats exposed to a novel, complex environment. Brain Res 339:361–365.

Tiesinga PH, Sejnowski TJ (2001) Precision of pulse-coupled networks of integrate-and-fire neurons. Network 12:215–233.

Varela JA, Sen K, Gibson J, Fost J, Abbott LF, Nelson SB (1997) A quantitative description of short-term plasticity at excitatory synapses in layer 2/3 of rat primary visual cortex. J Neurosci 17: 7926–7940.

Volkmar FR, Greenough WT (1972) Rearing complexity affects branching of dendrites in the visual cortex of the rat. Science 176:1445–1447.

Wang XJ (1998) Calcium coding and adaptive temporal computation in cortical pyramidal neurons. J Neurophysiol 79:1549–1566.

Zhu J, Apparsundaram S, Bardo MT, Dwoskin LP (2005) Environmental enrichment decreases cell surface expression of the dopamine transporter in rat medial prefrontal cortex. J Neurochem 93: 1434–1443.

APPENDIX

Pyramidal cell model

We represented the distribution of ionic currents across dendrites, soma and axon, in a three compartment pyramidal-cell model. The model includes the most relevant ionic conductances present in cortical pyramidal cells (Wang 1998): sodium (I_{Na}) current, delayed rectifier K^+ ($I_{K\text{-}dr}$) current, high-voltage activated Ca^{2+} (I_{Ca}) current, and a calcium-dependent K^+ current ($I_{K(Ca)}$). A coupling conductance (g_c) value regulates the current flow between dendrite and soma, and soma and axon. A slightly modified set of membrane conductances was used to describe interneuronal spiking. The somatic, dendritic, and axonal terminal membrane potentials V_s, V_d, and V_p are described by following equations

$$C_m\frac{dV_s}{dt}=-I_L-I_{Na}-I_K-I_{Ca}-I_{AHP}+I_{inject}-\frac{g_c}{p}(V_s-V_d)$$

$$C_m\frac{dV_d}{dt}=-I_L-I_{Ca}-I_{AHP}-\frac{g_{c1}}{(1-2^*p)}(V_d-V_s)-I_{AMPA}-I_{NMDA}$$

$$C_m\frac{dV_p}{dt}=-I_L-I_{Na}-I_K-I_{Ca}-I_{AHP}-\frac{g_{c2}}{p}(V_p-V_s)$$

where $C_m=1\ \mu F/cm^2$ and I_{inject} is the cosine function (in $\mu A/cm^2$).

Short-term plasticity in a glutamatergic synapse

The model contains four parameters representing the short-term dynamic of synaptic plasticity: facilitation (F), slow depression (DS), fast depression (DF) and initial amplitude (A_0). These four parameters are dependent on the intracellular calcium concentration. The change in response amplitude (A) is the product of these three parameters (Varela et al., 1997)

$$A=A_0\cdot F\cdot DS\cdot DF$$

$$I_{AMPA(or\ NMDA)}=A\cdot\alpha(V)\cdot(V-E)$$

where $\alpha(V)$ is an α-function

$$\alpha(t)=t\cdot e^{-t/\tau}$$

where the kinetics of the glutamatergic synaptic currents is contained in the decay time τ (Brunel and Wang, 2001; Tiesinga and Sejnowski, 2001).

(Accepted 27 December 2006)
(Available online 8 February 2007)